Antiphase Boundaries and Ordering Defects in Syndiotactic Polystyrene Crystals

Philippe Pradère† and Edwin L. Thomas*,‡

Polymer Science and Engineering, University of Massachusetts, Amherst, Massachusetts 01003

Received July 25, 1989

ABSTRACT: Syndiotactic polystyrene thin films were grown on a hot glycerol surface. Electron diffraction (ED) patterns obtained from monolayer areas show many high-order Bragg reflections suggesting well-developed long-range order as well as streaks of intensity indicating the presence of defects in the crystal lattice. These defects have been characterized in both real and reciprocal spaces by high-resolution electron microscopy (HREM). Optical diffractograms from selected areas (average radius 50 nm) of HREM images show in many cases new reflections in the form of sharp spot(s) and/or short streaks at positions where ED patterns give extended streaks. This additional scattering is shown to arise from small domains that can be imaged by optical filtering and image reconstruction on a laser bench. The domains are elongated and thin (less than 5 nm wide) and are interpreted as a new superstructure $sPS_{s''}$) by analogy with a recent model (a basic superstructure: $sPS_{s'}$) proposed for the rest of the crystal. The two superstructures $sPS_{s'}$ and $sPS_{s''}$ result from ordering between enantiomorphous pairs of molecular clusters, each of them containing three molecules. Periodic arrays of domains of ordering are separated by plane boundaries analogous to antiphase boundaries and give rise to new superlattice reflections. We discuss the generalization of ordering phenomena, which are already well-known in metallic alloys, to a certain class of polymer crystals.

Introduction

The recent synthesis of highly stereoregular (>98%) syndiotactic polystyrene (sPS)[1-3] has brought interest to this new material. sPS crystallizes very well and at a much faster rate than isotactic polystyrene, which has been known and extensively used for more than 30 years.[4] Various morphologies and different crystalline structures of sPS have been reported in the recent literature.[5-9] Petermann and colleagues[8,9] have given a first detailed description of the morphology of thin films of sPS grown on top of a hot orthophosphoric acid surface. They proposed a hexagonal model, sPS_b, for the unit cell based on electron diffraction data and suggested that, depending on crystallization conditions, ordering between enantiomorphous chain clusters leads to the formation of a superstructure $sPS_{s'}$. Furthermore, electron diffraction patterns contained streaks suggesting the presence of defects in the superstructure. Streaks and related defects have also been observed in single crystals of sPS characterized by an orthorhombic unit cell.[7,10]

The aim of the present work is to give a detailed description for the defects present in thin films of sPS using high-resolution electron microscopy (HREM) and microdiffraction. HREM permits study of the crystalline structure at a molecular level and is therefore particularly well suited for the characterization of defects.[11] Degradation related to electron beam irradiation can be minimized by using low-dose techniques, and many studies in the recent literature have shown the applicability of HREM for polymer physics (e.g., refs 12-15).

Experimental Section

1. **Specimen Preparation.** Syndiotactic polystyrene, M_w = 157 000 (Idemitsu Kosan Co., Ltd., Japan), is first dissolved in xylene. One drop of the solution is deposited on top of a hot glycerol surface (T > 240 °C), where it spreads and crystallizes when the glycerol is cooled to room temperature. The film is then floated onto water in order to dissolve the glycerol. Samples from the thinnest part are collected onto thin carbon-coated (5-8 nm) grids (400 mesh) for electron microscopy.

2. **Electron Microscopy.** Electron microscopy is performed on a Jeol 2000 FX (200 kV, C_s = 2.3 mm) equipped with a Gatan camera and a built-in minimum-dose system (MDS). The MDS allows set up of high-resolution conditions with minimum sample irradiation prior to imaging. The total end point dose (TEPD), measured by timing under known beam current densities the complete disappearance of all crystalline peaks in an electron diffraction pattern, is approximately 175 C/m². For Kodak SO163 film developed 10 min in full-strength D19 developer, the highest magnification possible for imaging can be calculated as follows:

$$M_{max} = (D_{max}/D_{film})^{0.5}$$

where D_{max} is the actual dose used for imaging (typically 50-75% of the TEPD) and D_{film} is the dose necessary to expose the film with an optical density of 0.5. This value of 0.5 was found by experience to be an optimum between film contrast and sample degradation. With D_{max} = 100 C/m² and $D_{film} = 0.5 \times 10^{-9}$ C/m² (Kodak data release), we obtain M_{max} = 45 000. In order to further reduce the irradiation dose and because only discrete magnification values are available, we selected a magnification of 41 000.

Two defocus conditions have been selected: (1) At 50-nm overfocus the image represents directly the projected potential of the material up to a resolution of ca. 0.5 nm (which is enough to properly transfer all 24 strongest reflections of the diffraction pattern). In this case the defocus can be directly measured from an optical diffractogram of the negative. (2) At 90-nm underfocus (the Scherzer focus) the image also well represents the projected potential, with a negative contrast and with a better resolution (up to 0.3 nm), but the precise defocus value is not directly measurable from the image negative. Because a particular defocus value cannot be selected with precision in the MDS mode (the error estimate is ±50 nm for a magnification of 41 000), image details at resolutions better than 0.5 nm cannot be reliably interpreted unless the image defocus can be measured with precision. Also due to the sensitivity of sPS to irradiation, optical diffractograms show very few reflections between 0.3 and 0.5 nm (for the images obtained under the conditions previously mentioned).

3. **Optical Image Processing.** HREM images are checked on a laser bench where an optical diffraction (OD) pattern can be obtained.[11,16,17] An OD pattern shows the same information as an electron diffraction (ED) pattern but with a lower resolution

† Centre d'Etudes Nucléaires, SCMM/D.LETI, Bât C4, 38041 Grenoble Cedex, France.
‡ Department of Materials Science and Engineering, MIT, Cambridge, MA 02139.

0024-9297/90/2223-4954$02.50/0

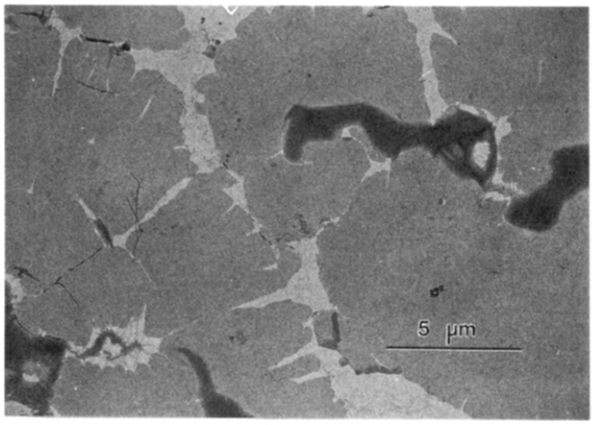

Figure 1. Bright-field image of a thin area of a sPS film grown on a hot glycerol surface. Irregular growth features are observed but uniform monolayers exist over several micrometers.

because it is attenuated by the point transfer function (PTF) of the microscope. OD patterns, however, can originate from a much smaller area than ED patterns (typically 50-nm radius instead of 0.5 μm) so that they permit examination of the crystal structure at a much smaller scale. Depending on defocus conditions, OD patterns also show in some cases the modulation of the continuous object frequency spectrum from the carbon support film due to the PTF and which can be used to calculate the defocus value.[16] The optical bench is also used for image filtering by selecting with a mask one or more OD spots and reconstructing an image that evidences the areas from which the selected spots had originated in a manner similar to dark-field imaging in the electron microscope. Because of many limitations of the technique (lens aberrations, filter alignment, convolution effects due to filtering, etc.) such reconstructed images cannot be interpreted in fine detail but do give a reasonable idea of the size and shape of regions in the image giving rise to that portion of the OD pattern selected by the mask.

Results and Discussion

1. Morphology of sPS Films. Figure 1 shows a bright-field image obtained from a thin section of a sPS film grown on a hot glycerol surface. A typical film contains multilayer regions giving rise in electron diffraction to multiple spots due to slight misorientations between layers. Also thicker areas show the presence of edge-on lamellae as described elsewhere.[9] However, in Figure 1, which represents one of the few such parts of the film, monolayers of uniform thickness are observed over large distances, up to 5-μm diameter in this case. Irregular growth patterns are observed at the edges of the uniform parts of the monolayer and are probably the result of the high rate at which the film crystallized. Unfortunately, the sample was not crystallized under well-controlled conditions. Attempts to prepare single crystals by self-seeding have therefore given poor results (low-crystallinity lamellae). It is of future interest to address these problems in order to have a more reproducible sample preparation and to explore the influence of crystallization conditions on sample ultrastructure.

Electron diffraction patterns from the monolayer regions show a high crystallinity (Figure 2). This pattern can be indexed with the hexagonal superstructure model as proposed by Greis et al.[9] In this model, later referred as "superstructure s'" or $sPS_{s'}$, sPS chains with a planar zigzag conformation pack three by three into clusters that, by shifts of $c/2$ along the chain axis, order to form enantiomorphous pairs. The enantiomorphous relationship is the basic reason for the large hexagonal superstructure unit cell (space group $P\bar{6}2c$) with parameters $a = 2.626$ nm and $c = 0.5045$ nm and containing 9 chains.[9]

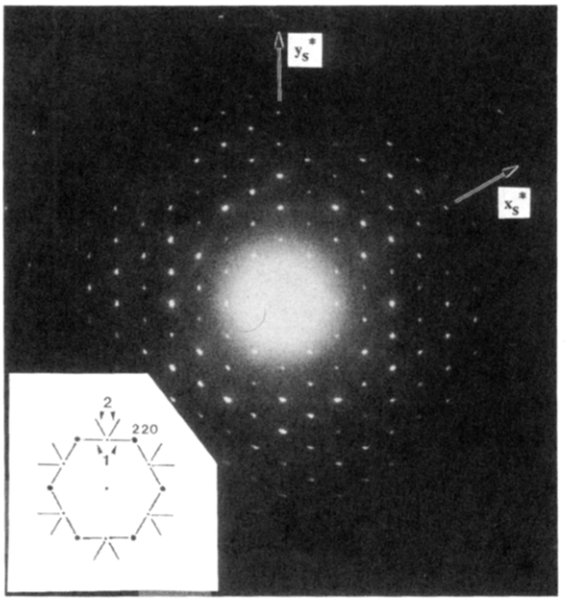

Figure 2. (a) Electron diffraction pattern obtained from a monolayer film of sPS. Streaks indicating the presence of defects appear at several locations. The insert shows schematically the streak positions (labeled 1 and 2) with respect to the most intense ED reflections: 220 and 300.

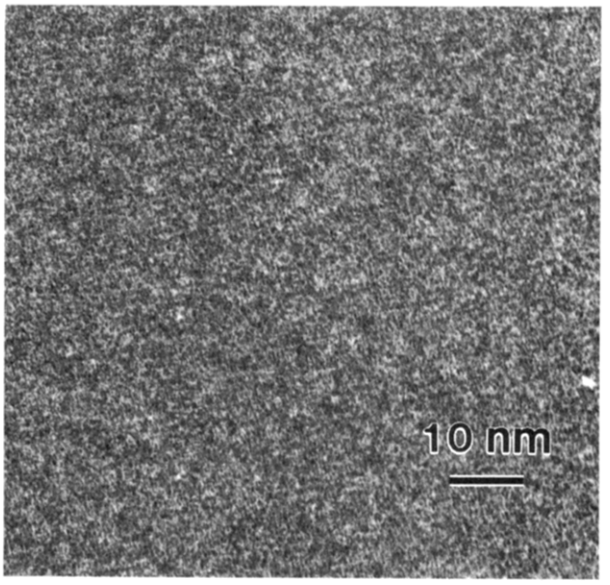

Figure 3. High-resolution image obtained from a monolayer sPS lamella at a defocus close to Scherzer. The detailed information contained in this image is best analyzed in optical diffractograms (see next figures).

An interesting feature of these electron diffraction patterns is the presence of streaks at specific locations. The most intense streaks form a hexagon joining the six most intense spots of the pattern: the 220 spots (see Figure 2). These streaks and others less intense are represented in Figure 2 (insert). They indicate the presence of defects in the crystal that will be characterized in the following section by high-resolution electron microscopy. Indeed, the morphology of these films, thin and uniform over large distances, and their high crystallinity are an advantage for the use of the HREM technique.

2. High-Resolution Imaging. Figure 3 shows a HREM image obtained from a monolayer. Three sets of fringes oriented at 60° one from another and corresponding to a spacing of 1.3 nm (110 planes) can be seen. Lines with half this spacing (220 planes) together with some fine structural detail can be seen by observing the image

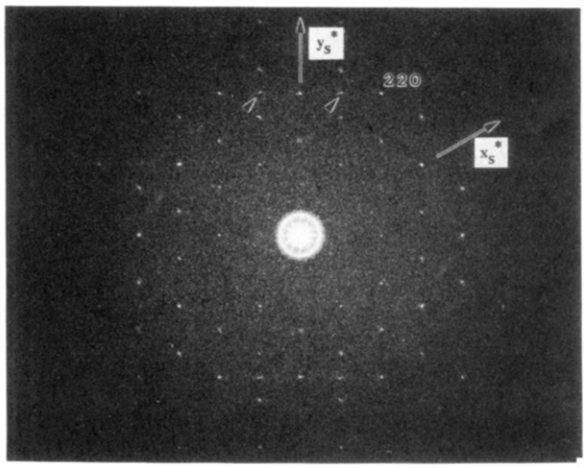

Figure 4. Optical diffractogram obtained from a HREM image such as Figure 3 showing information up to 0.44 nm (330 spot). Single spots are observed (arrows) instead of streaks. Note that the intensity of these extra spots can be compared to the other strong spots.

at a glancing angle. A direct interpretation of such an image is difficult due to its low contrast and moreover to the complexity of the crystal packing. Individual sPS molecules have a "spread" c-axis projected potential since the phenyl rings lie on opposite sides of the planar zigzag main chain so that the molecules cannot be simply identified on the image as a single circular region.

One way to investigate the fine details of the structure that might be included in the image is to retrieve its optical diffractogram. Figure 4 is such an example obtained from a selected area of an image similar to Figure 3. Most of the spots present in the ED pattern (Figure 2) below a resolution of 0.5 nm are observed in the OD pattern. The diffraction pattern originates from a very small area (diameter of 100 nm in this case but the region can be as small as 50 or 25 nm) and therefore permits investigation of the crystal structure at a very local scale.

One difference that appears clearly by comparison of OD's with ED's is the absence of streaks, especially those between the 220 spots, which are the most intense in the ED pattern. Instead, OD patterns show single spots (arrowed in Figure 4) at a position that corresponds to the center of the ED streak (Figure 2). This position is also the midpoint of the nearest-neighbor spots: 220 and 300. Other OD patterns obtained under similar conditions have shown these extra spots more elongated, indicating that they originate from a domain having one very small dimension. Similar spots have also been observed at the center of streaks 2. These extra spots suggest the existence of domains with a different crystal structure. These domains are of very small dimensions for the following reasons: (1) when the laser beam is moved over the HREM negative, extra spots are only observed for a few small areas; (2) the extra spots show a small amount of streaking.

The size of the domains associated with the extra reflections can be crudely estimated by varying the size and moving the aperture used to select an area for optical diffraction on the negative. From these experiments we conclude that the domains are very small and never extend over more than a few hundred nanometers. In order to give a more quantitative description, we performed optical filtering on a laser bench. When extra spots revealing the presence of a domain are detected on the OD pattern, a filter selecting only these spots is introduced in the OD plane and an image is reconstructed. Such reconstructions are shown in Figure 5 and confirm our hypothesis of thin domains. The domains appear straight and elongated

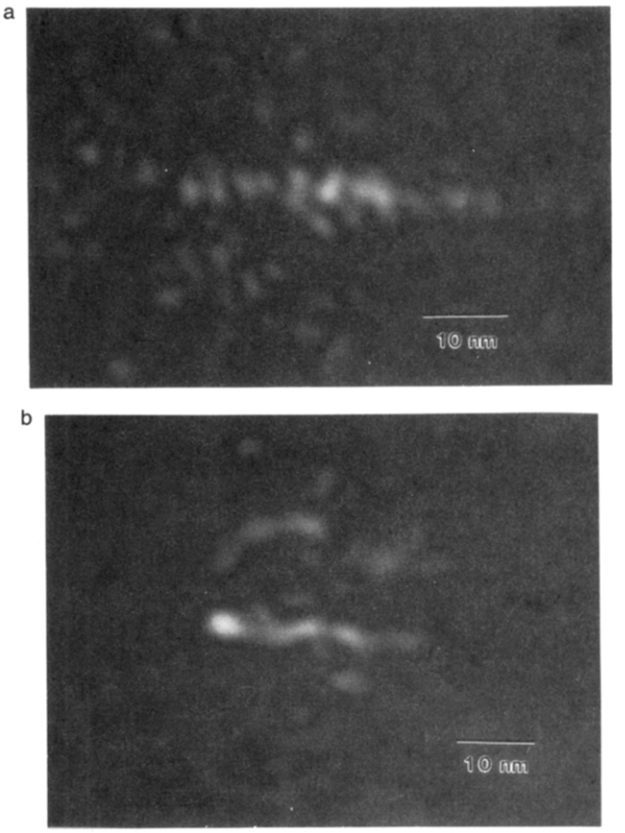

Figure 5. Filtered images showing thin and elongated domains representing a new superstructure $sPS_{s''}$: (a) one single domain; (b) two domains roughly parallel. These domains have been imaged by filtering type 1 reflections (see text and insert of Figure 2).

along the x axis with a thickness of ca. 5 nm for a length of up to 100 nm. Figure 5b shows two domains running parallel to each other. Note that the fine structure observed in the reconstructed image of the domains is just an interference pattern created by the filtering process and should be ignored.

From the position of the extra spots in the OD pattern, a new superstructure (denoted s'') can be proposed as described in Figure 6a. The new reciprocal unit cell ($a_{s''}$*, $b_{s''}$*) results from an alternate arrangement of the basis hexagonal cell of sPS_b into a new superstructure $sPS_{s''}$. $a_{s''}$* and $b_{s''}$* are obtained by a 30° rotation of $a_{s'}$* and $b_{s'}$* and are also half the unit vectors of the basis reciprocal cell, a_b* and b_b*. OD patterns such as Figure 4 therefore represent a mixture of two patterns, one coming from a $sPS_{s''}$ domain that includes the extra spot and the other from the surrounding $sPS_{s'}$ crystal. Because domains are very thin and long, it is not possible to isolate their contribution from the surrounding crystal by using a circular aperture for selection. Figure 6a shows in reciprocal space the three different unit cells of sPS_b, $sPS_{s'}$, and $sPS_{s''}$. A schematic of the molecular arrangements around a domain is given in Figure 6b together with the unit cells corresponding to the two superstructures.

Assuming that the new superstructure results from ordering between enantiomorphous clusters by $c/2$ shifts along the molecular axis, as described for the superstructure $sPS_{s'}$,[9] possible unit cells can be drawn by placing either "up" (shifted $c/2$ up) or "down" (shifted $c/2$ down, relative to the "up") clusters at the basis hexagonal cell positions of sPS_b inside the $sPS_{s''}$ unit cell. Considering all symmetrically equivalent configurations, only one unit cell compatible with the lattice vectors exists and is represented

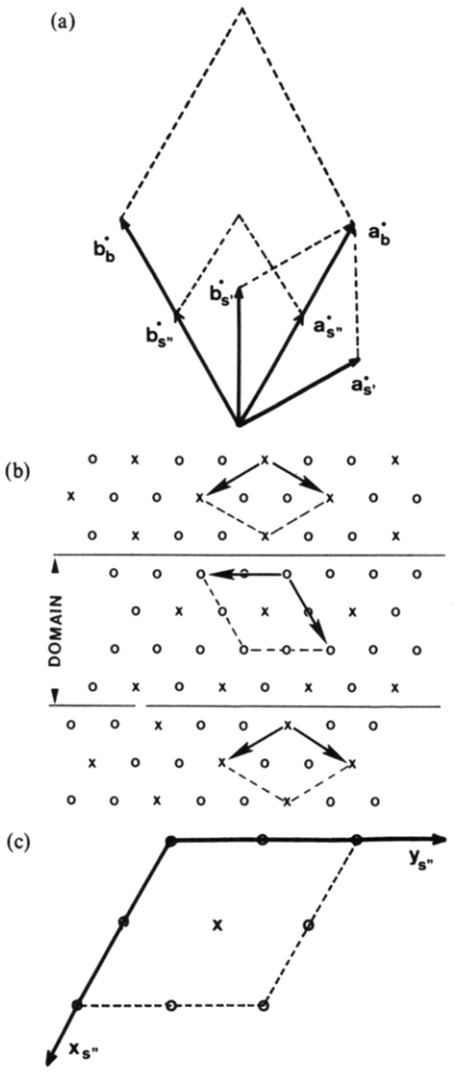

Figure 6. (a) Schematic showing superstructure unit cells in reciprocal space. The basic hexagonal unit cell is also given for reference. (b) Schematic showing a domain with its new superstructure unit cell. (c) Given two sorts of clusters (O and × represent the "up" and "down" clusters), only this configuration is possible for the new unit cell.

in Figure 6b. The O and × signs relate to the "up" and "down" clusters. It is interesting to notice here that the local environment of the "down" (the "×") is the same as in the basic superstructure: the six first neighbors are all "up". This same local configuration might explain why this new superstructure exists although it might be energetically less stable.

Using HREM we have been able to characterize domains large enough so that their contribution in diffraction (OD) can be detected. Smaller domains, and more especially thinner ones, are also expected to exist more frequently and contribute to the streaks observed in ED patterns. The new superstructure does not likely correspond to a lower energy but occurs probably because of the very fast and nonisothermal crystallization process.

3. Antiphase Boundaries. Some OD patterns such as Figure 7a contain extra reflections but in this case, instead of a single spot, a pair of spots is observed (arrowed in Figure 7a) at position 1 (as defined in Figure 2). Such a pair is also present in Figure 7b where it appears centered on position 2. These pair of spots appear at both positions 1 and 2 and are aligned with the corresponding ED streak direction. Their midpoints correspond precisely to positions 1 and 2. The superstructure $sPS_{s''}$ that was

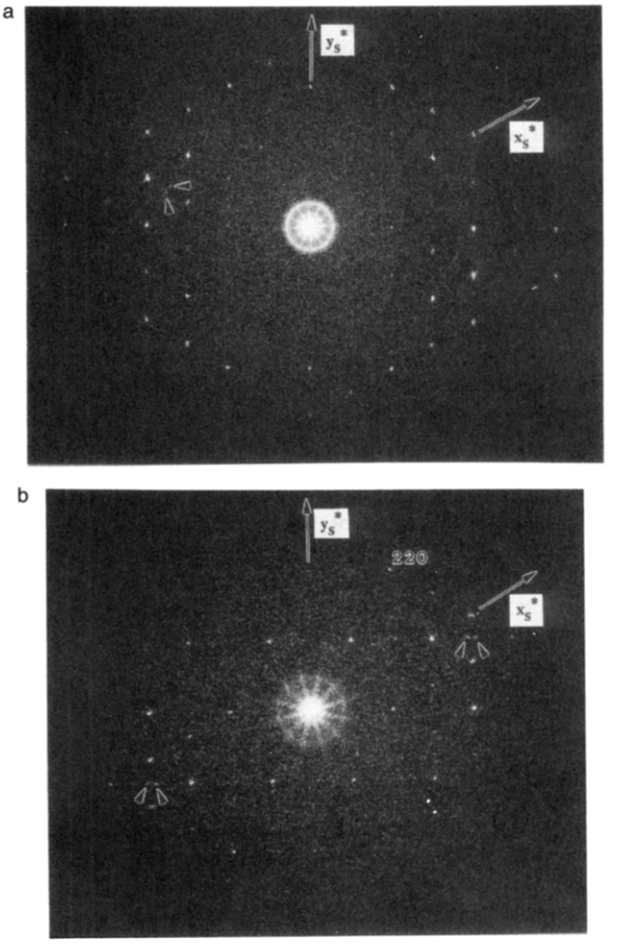

Figure 7. OD pattern showing a pair of extra spots instead of one single extra spot: (a) at position 1; (b) at position 2.

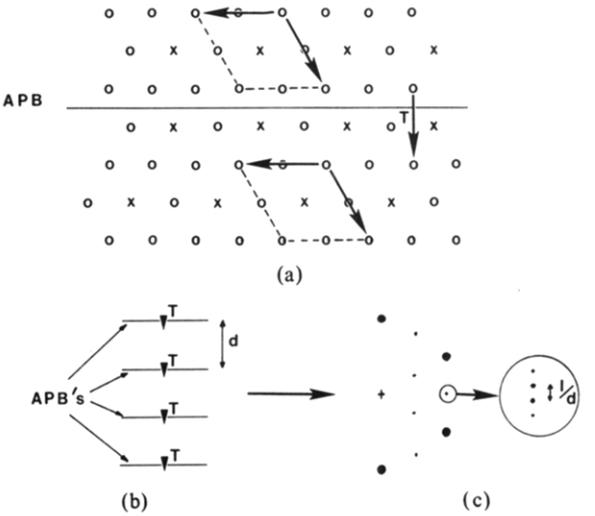

Figure 8. (a) Schematic representation of an antiphase boundary in the new $sPS_{s''}$ superstructure. The defect is obtained by exchanging the positions of O ("up") and × ("down") clusters at the boundary. (b) A periodic array of such defects results in a diffraction pattern in (c) that explains the extra pair of spots observed for $sPS_{s''}$ in Figure 7.

proposed to account for the presence of single spots is not sufficient to explain their splitting. An evolution from the continuous superstructure can be proposed as follows in order to explain the pair of spots.

Figure 8a shows, adapted to the case of sPS clusters, a characteristic ordering defect commonly present in ordered alloys: an antiphase boundary. Such a defect is created in an AB ordered alloy (e.g., A might be a gold atom and

B a copper atom as Au–Cu alloys typically form APB's[18]) by exchanging across a plane, the antiphase boundary, the A and B positions. In Figure 8a the A and B moieties are the "up" (O) or "down" (×) sPS clusters. The two crystal domains separated by the plane are therefore related by a translation (T) that does not belong to the lattice in a similar way as the displacement due to a stacking fault. Now if we consider a periodic array of such boundaries as represented in Figure 8b, the contribution to the diffraction pattern can be calculated (see, for instance, ref 18) and is given in Figure 8c. This pattern shows a striking analogy with what we have observed in the OD pattern from sPS: a pair of new spots (with possibly weaker higher orders) is observed instead of a single new reflection corresponding to the superstructure. The distance between spots gives the spacing between antiphase domains.[18] From Figure 8a,b this spacing is ca. 10 nm. Such a distance seems to indicate the existence of larger domains than in Figure 5. These domains have not been successfully imaged by filtering due to the weakness of the spots.

4. Discussion. Ordering between clusters of different handedness was suggested to explain the crystalline structure of syndiotactic polystyrene.[9] Our HREM results indicate that ordering phenomena in this material can be generalized and lead to the creation of domains that can be compared to well-known phenomena occurring in metallic alloys. Antiphase boundaries are one kind of such defect that was investigated here by OD. To our knowledge, PVF2 is the only polymer where antiphase boundaries have been previously observed.[19,20] The existence of such defects related to ordering between chains of different symmetry needs more clarification, especially in order to determine under which conditions such defects occur.

Ordering into domains of well-defined boundaries was evidenced in the case of poly(4-methyl-1-pentene) single crystals and tentatively explained by a segregation of right- and left-handed helices.[21] As we have observed for sPS, the domain boundaries were also straight. This further points out the possible generalization of ordering defects to polymer crystals with chains or chain clusters having different handedness [e.g., helical conformation such as poly(4-methyl-1-hexene)[22] or even poly(1-butene) or polypropylene].

Our HREM study has also demonstrated another aspect of the technique that is very useful in the case of polymers for which noisy images are obtained. For a complex crystalline structure a direct interpretation of HREM image is very difficult and furthermore depends on the exact defocus at which the micrograph is taken, which is only known approximately. Optical diffractograms depend less strongly on defocus and permit one to study the crystal structure in a similar way to electron diffraction but without the time constraints due to beam degradation (which was a constraint only during the HREM imaging process) and with a spatial resolution on the sample of at least an order of magnitude better.

Acknowledgment. We thank Prof. J. Petermann for initiating this research. This work was supported by AFOSR Grant 88001.

References and Notes

(1) Ishihara, N.; Seimiya, T.; Kuramoto, M.; Uoi, M. *Macromolecules* **1986**, *19*, 2465.
(2) Pellecchia, C.; Longo, P.; Grassi, A.; Ammendola., P.; Zambelli, A. *Makromol. Chem., Rapid Commun.* **1987**, *8*, 277.
(3) Oliva, L.; Pellecchia, C.; Cinquina, P.; Zambelli, A. *Macromolecules* **1989**, *22*, 1642.
(4) Natta, G.; Pino, P.; Corradini, P.; Danusso, F.; Mantica, E. *J. Am. Chem. Soc.* **1955**, *77*, 1700.
(5) Chatani, Y.; Fuji, Y.; Shimane, Y.; Ijitsu, T. *Polym. Prepr. Jpn.* **1988**, *37*, (4), 1179.
(6) Kobayashi, M.; Nakaoki, T.; Uoi, M. *Polym. Prepr. Jpn.* **1988**, *37* (4), 1187.
(7) Tosaka, M.; et al. *Polym. Prepr. Jpn.* **1988**, *37* (4), 1183.
(8) Greis, O.; Asano, T.; Xu, Y.; Petermann, J. *Z. Kristallogr.* **1988**, *182*, 58.
(9) Greis, O.; Asano, T.; Xu, Y.; Petermann, J. *Polymer* **1989**, *30*, 590.
(10) Tosaka, M.; Tsuji, M.; Kawagushi, A.; Katayama, K.-I.; Iwatsuki, M. *Polym. Prepr. Jpn.* **1988**, *37* (8), 2564.
(11) Neumann, W.; Pasemann, M.; Heydenrich, J. *Crystals, Growth, Properties and Applications*; Springer: Berlin, 1982, 1.
(12) Tsuji, M.; Isoda, S.; Ohara, M.; Kawagushi, A.; Katayama, K.-I. *Polymer* **1982**, *23*, 1568.
(13) Revol, J.-F.; Manley, R. St. J. *J. Mater. Sci., Lett.* **1986**, *5* 249.
(14) Pradère, P.; Revol, J.-F.; Nguyen, L.; Manley, R. St. J. *Ultramicroscopy* **1988**, *25*, 69.
(15) Pradère, P.; Thomas, E. L. *Philos. Mag. A* **1989**, *60* (2), 177.
(16) Krivanek, O. L. *Optik* **1976**, *45*, 97.
(17) Spence, J. C. H. *Experimental High Resolution Electron Microscopy*; Clarendon Press: Oxford, 1981, p 266.
(18) Hirsch, P. B.; Howie, A.; Nicholson, R. B.; Pashley, D. W.; Whelan, M. J. *Electron Microscopy of Thin Crystals*; Butterworth: London, 1965; pp 354, 382.
(19) Takahashi, Y.; Matsubara, Y.; Tadokoro, H. *Macromolecules* **1983**, *16*, 1588.
(20) Takahashi, Y.; Tadokoro, H. *Polym. J.* **1983**, *15*, 733.
(21) Pradère, P.; Revol, J.-F.; Manley, R. St. J. *Macromolecules* **1988**, *21*, 2747.
(22) Bassi, I. W.; Bonsignori, O.; Lorenzi, G. P.; Pino, P.; Corradini, P.; Temussi, P. A. *J. Polym. Sci., Part A-2* **1971**, *9*, 193.

Registry No. sPS, 28325-75-9.